



In vitro trypanocidal potency and *in vivo* treatment efficacy of oligomeric ethylene glycol-tethered nitrofurantoin derivatives

Helena D. Janse van Rensburg^{a,*}, David D. N'Da^{a,1}, Keisuke Suganuma^{b,1}

^a Centre of Excellence for Pharmaceutical Sciences, North-West University, Potchefstroom 2520, South Africa

^b National Research Center for Protozoan Diseases, Obihiro University of Agriculture and Veterinary Medicine, Inada, Obihiro, Hokkaido 080-8555, Japan

ARTICLE INFO

Keywords:

African trypanosome
Trypanocidal potency
Nitroheterocycle
Nitrofurantoin
Ethylene glycol

ABSTRACT

African trypanosomiasis is a significant vector-borne disease of humans and animals in the tsetse fly belt of Africa, particularly affecting production animals such as cattle, and thus, hindering food security. *Trypanosoma congolense* (*T. congolense*), the causative agent of *nagana*, is livestock's most virulent trypanosome species. There is currently no vaccine against trypanosomiasis; its treatment relies solely on chemotherapy. However, pathogenic resistance has been established against trypanocidal agents in clinical use. This underscores the need to develop new therapeutics to curb trypanosomiasis. Many nitroheterocyclic drugs or compounds, including nitrofurantoin, possess antiparasitic activities in addition to their clinical use as antibiotics. The current study evaluated the *in vitro* trypanocidal potency and *in vivo* treatment efficacy of previously synthesized anti-leishmanial active oligomeric ethylene glycol derivatives of nitrofurantoin. The trypanocidal potency of analogues **2a-o** varied among the trypanosome species; however, *T. congolense* strain IL3000 was more susceptible to these drug candidates than the other human and animal trypanosomes. The arylated analogues **2k** (IC₅₀ 0.04 μM; SI >6365) and **2l** (IC₅₀ 0.06 μM; SI 4133) featuring 4-chlorophenoxy and 4-nitrophenoxy moieties, respectively, were revealed as the most promising antitrypanosomal agents of all analogues against *T. congolense* strain IL3000 trypomastigotes with nanomolar activities. In a preliminary *in vivo* study involving *T. congolense* strain IL3000 infected BALB/c mice, the oral administration of 100 mg/kg/day of **2k** caused prolonged survival up to 18 days post-infection relative to the infected but untreated control mice which survived 9 days post-infection. However, no cure was achieved due to its poor solubility in the *in vivo* testing medium, assumably leading to low oral bioavailability. These results confirm the importance of the physicochemical properties lipophilicity and water solubility in attaining not only *in vitro* trypanocidal potency but also *in vivo* treatment efficacy. Future work will focus on the chemical optimization of **2k** through the investigation of analogues containing solubilizing groups at certain positions on the core structure to improve solubility in the *in vivo* testing medium which, in the current investigation, is the biggest stumbling block in successfully treating either animal or human *Trypanosoma* infections.

1. Introduction

African trypanosomiasis (AT) is mainly caused by three *Trypanosoma* (*T.*) species, namely *T. brucei*, *T. congolense*, and *T. vivax* (Barr et al., 2014). These salivarian eukaryotic flagellates are cyclically transmitted through the bite of hematophagous tsetse flies (*Glossina* species) which are only found in Africa, specifically in the savannahs and woodlands of sub-Saharan Africa (Barr et al., 2014; Blowey and Weaver, 2011; Pays et al., 2023). *Trypanosoma brucei* (*T. b.*) subspecies include *T. b. brucei*, *T. b. gambiense*, and *T. b. rhodesiense* which are morphologically

indistinguishable and referred to as “*T. brucei* complex” organisms (Barr et al., 2014). *T. b. gambiense* and *T. b. rhodesiense* cause “sleeping sickness” in humans in West and East Africa, respectively (Barr et al., 2014; Nok, 2009; Pays et al., 2023). The slow-progressing Gambian trypanosomiasis, responsible for >95 % of cases, is an anthroponotic disease involving human-to-human transmission, and as such, anti-trypanosomiasis campaigns focused on diagnosis and treatment (Pays et al., 2023). Consequently, its incidence has declined to less than 1 000 cases per year; nevertheless, more than 50 million people in 36 sub-Saharan African countries remain at risk of infection (WHO, 2023).

* Corresponding author.

E-mail address: 23551917@mynwu.ac.za (H.D. Janse van Rensburg).

¹ David D. N'Da and Keisuke Suganuma contributed equally.

The fast-progressing Rhodesian trypanosomiasis, responsible for <5 % of cases, is a zoonotic disease involving animal-to-human transmission, and can result in unpredictable disease outbreaks (Pays et al., 2023). The mammalian immune system is unable to provide efficient protection against trypanosomal infection (Pays et al., 2023); since trypanosomes have developed strategies to continuously escape innate and adaptive host immune responses by changing their surface coat. Thus, a vaccine against AT is unlikely (Horn, 2014). Furthermore, available therapies for sleeping sickness are deficient in efficacy, safety, or both (Giordani et al., 2016; Imran et al., 2022; Sokolova et al., 2010; Venturelli et al., 2022). The accessibility to these therapies is also of concern (Sokolova et al., 2010).

Trypanosoma b. brucei, *T. congolense*, and *T. vivax* species cause disease in a variety of domestic and wild animals (either alone or in combination), but do not infect humans (Barr et al., 2014) due to the trypanolytic activity of membrane pore-forming apolipoprotein I-I found in human blood (Pays et al., 2023; Vanhamme et al., 2003). Animal AT (“nagana”) is one of the most significant vector-borne diseases in the humid and sub-humid tropics of Africa, (Katabazi et al., 2021; Morrison et al., 2016; Muhanguzi et al., 2014), which affects animals in an area one-third larger than that of the United States of America (USA) (Morrison et al., 2016). It causes the death of more than 3 million animals each year with 50 million animals at risk of infection (Chitanga et al., 2011; Coustou et al., 2010), leading to losses of between 1.5 and 5 billion US dollars per year (Blowey and Weaver, 2011). Therefore, animal AT is the main hindrance to food security, as it makes vast areas of semiarid savannah land in Africa unsuitable for breeding domestic animals that are a source of food (Chitanga et al., 2011; Katabazi et al., 2021). Such limitations on livestock production lead to shortages of meat, milk, draught animals, and manure (Shaw et al., 2015; Swallow, 2000). The presence of AT also hinders the export of livestock and their products to developed countries (Shaw et al., 2015; Swallow, 2000). In terms of severity and consequences for productivity, *T. congolense* strain Il3000 (also known as the Savannah subtype) is the main causative agent of animal AT in East Africa, particularly affecting cattle (Desquesnes et al., 2022; Giordani et al., 2016; Venturelli et al., 2022). Additionally, it has a large wildlife host reservoir that seems tolerant to infection, and thus, parasite eradication appears to be impossible (Pays et al., 2023).

T. evansi (the causative agent of “surra” in animals) is very closely related to *T. brucei* and may have derived from it as a result of partial or complete loss of kinetoplast DNA; which stops *T. evansi* from developing within the insect vector (Blowey and Weaver, 2011). Thus, it has adapted to mechanical transmission by hematophagous insects, such as horse (*Tabanus* species) and stable (*Stomoxys* species) biting flies during an interrupted blood meal (Blowey and Weaver, 2011). Consequently, it has spread beyond the tsetse transmission zone in sub-Saharan Africa to become the most widely distributed animal trypanosome, affecting the livestock industries in North and Northeast Africa, Latin America (except Chile), the Middle East, and Asia (Borges et al., 2014). *T. equiperdum* (the causative agent of “dourine” in equines) also shares a phylogenetic relationship with *T. brucei*; however, it is sexually transmitted among equines (Cayla et al., 2019; Desquesnes et al., 2022; Giordani et al., 2016). It is prevalent in Africa, the Middle East, and Central and South America (Paccamonti and Crabtree, 2019).

Chemotherapy for AT in domestic animals depends on only a few compounds, of which several are chemically related; for example, ethidium bromide, isometamidium chloride, and diminazene aceturate (Kasozi et al., 2022; Peregrine and Mamman, 1993) (Fig. 1). The latter two agents cannot penetrate the blood-brain barrier (BBB), which is problematic in the management of *T. brucei* complex organisms who reside outside the circulatory system of their mammalian host (Giordani et al., 2016). Increased drug resistance, particularly to isometamidium chloride and diminazene aceturate, is concerning because it implies that these drugs’ future usefulness may be compromised (Kasozi et al., 2022). Another key concern is drug safety, specifically residues in production animals (Wilkowski, 2022).

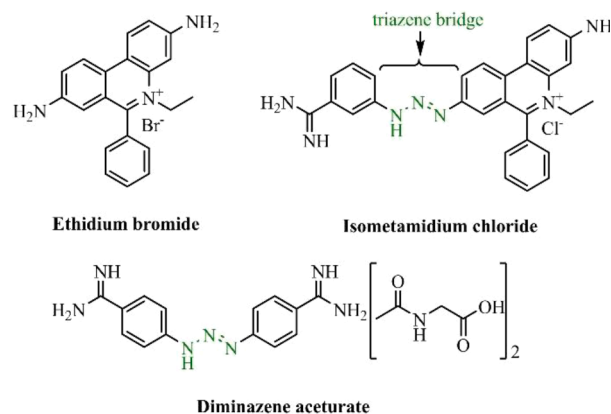


Fig. 1. Structures of veterinary trypanocidal agents in clinical use.

De novo drug discovery is a highly rational approach, but this process is not only extensive but also expensive (Hughes et al., 2011; Kaiser et al., 2015; Royle et al., 2013). Drug repurposing is another promising strategy used in drug discovery that identifies new therapeutic opportunities for existing drugs (Doan et al., 2011). Thus, when new drug applications are identified, these drugs or drug-like molecules can be rapidly advanced into clinical trials (Sahoo et al., 2021; Zhan et al., 2022) since they often have known pharmacokinetics, and safety profiles and are approved by the regulatory authorities (Chong and Sullivan, 2007; Kaiser et al., 2015; Weisman et al., 2006).

Nitroheterocyclic compounds have generally been avoided by the pharmaceutical industry; however, antitrypanosomal agents like nifurtimox and fexinidazole (Fig. 2) have re-ignited interest in nitroaromatics. The regimen combining nifurtimox, a sulfone-containing 5-nitrofuran, and eflornithine (NECT: nifurtimox-eflornithine combination therapy) is used to treat both stages of *T. b. gambiense* infection in humans (WHO, 2023). The orally bioavailable 2-substituted 5-nitroimidazole, was recently approved for the treatment of early and late-stage *T. b. gambiense* infection (Deeks, 2019). Additionally, the nitrofuran furazolidone (Fig. 2) has been widely used as an antibacterial and antiprotozoal feed additive for poultry, cattle, and farmed fish (Hu et al., 2007; Kaiser et al., 2015). Nitrofurans exert their biological activities through two environment-specific mechanisms of action involving the nitro group present in the nitrofuran synthon (Zhou et al., 2012). These include nitroreduction type I (NTR-I) which occurs under anaerobic conditions, and nitroreduction type II (NTR-II) which takes place in an aerobic environment (Trukhacheva et al., 2005; Zhou et al., 2012). Both mechanisms are catalyzed by pathogen-specific nitroreductase (Roldán et al., 2008) and result in the generation of toxic molecular species, such as nitroso, hydronitroso, and hydroxylamine in NTR-I (Ryan, 2017), and reactive oxygen species (ROS), for example, superoxide ion radicals ($\cdot\text{O}_2$) and hydroxyl radicals ($\cdot\text{OH}$) in NTR-II (Gutteridge, 1985; Wardman, 1985), which ultimately cause parasite death by oxidative stress (Gallardo-Garrido et al., 2020). The nitrofuran scaffold is among the privileged pharmacophores and has been proven to be highly effective in treating infectious diseases of bacterial origin. Indeed, nitroreductase is normally associated with bacteria and is absent from most eukaryotes, with trypanosomes being a major exception (Hall et al., 2010). Thus, the presence of crucial enzymes and/or metabolic pathways in the pathogen and lack thereof in humans, as well as the broad-spectrum activity against a wide variety of pathogens emphasizes that nitrofuran drugs (containing a redox-active scaffold) can play a significant role in the development of new chemotherapeutic agents (Blass, 2015; Zuma et al., 2019). Yet, the potential for drug repurposing of any nitrofuran for AT depends on their genotoxicity and/or mutagenicity relative to their efficacy in relevant rodent models (Kaiser et al., 2015).

Nitrofurantoin (NFT) is a synthetic nitrofuran that is administered

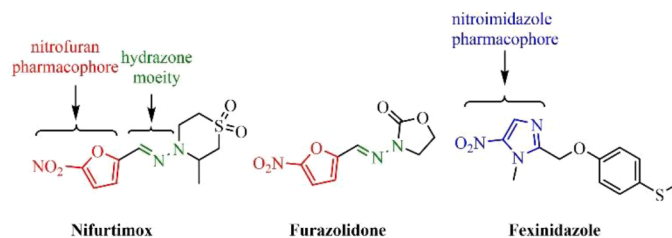


Fig. 2. Structures of nitroaromatic antiparasitic agents in clinical use.

orally for the prevention or treatment of urinary tract infections in humans as well as companion animals such as cats and dogs (extra-label use) (Mercer, 2022). Notably, the extra-label use of nitrofurans in production animals is prohibited; due to the residual carcinogenic, mutagenic, and/or teratogenic effects of these drugs in humans (Vass et al., 2008). The chemotherapeutic effects of nitrofurans are linked to the 5-nitrofurans moiety, whereas toxic properties are attributed to the hydrazone moiety, and by extension, to its non-nitro metabolites (Walzer et al., 1991). The azo bond of the diazenyl functional group can be reduced by azoreductase into active primary metabolites that can covalently bind to cellular proteins (Bendford et al., 2015; Ryan, 2017). Notably, the veterinary trypanocidal agents isometamidium chloride and diminazene aceturate contain a structurally related triazene bridge (Fig. 1). Despite their potential toxicity, the development of parasitic resistance against nitrofurans is rare as these drugs target multiple metabolic pathways, including carbohydrate and protein synthesis, DNA replication, and transcription (Zuma et al., 2019). Consequently, NFT may be a practical candidate for drug repurposing.

NFT, a Schiff base derived from 5-nitrofuralddehyde, is structurally related to the trypanocidal agent nifurtimox and shows hit trypanocidal activity against human and animal trypanosomes ($0.36 \mu\text{M} > \text{IC}_{50} < 1.96 \mu\text{M}$) (Kaiser et al., 2015; Munsimbwe et al., 2021). Derivatization of NFT at the α -N resulted in *n*-alkyl or aryl synthesized analogues with increased trypanocidal activity compared to the parent drug, with analogues containing 11- and 12-carbon aliphatic chains showing the highest trypanocidal activity ($\text{IC}_{50} < 0.34 \mu\text{M}$) and the lowest cytotoxicity ($\text{IC}_{50} > 246.02 \mu\text{M}$) *in vitro* (Munsimbwe et al., 2021). A 100 % survival and cure of *Trypanosoma congolense* IL3000 infected BALB/c mice were achieved with a minimum dose of 30 mg/kg nitrofurantoin per day for seven days (Suganuma et al., 2022), whereas the aforementioned analogues showed no treatment efficacy because they were insoluble in the *in vivo* testing medium (Munsimbwe et al., 2021). Thus, these results indicated that NFT analogues with high hydrophilicity were required for *in vivo* assessment. Other studies evaluated the trypanocidal activity of novel NFT analogues against the second major species of the *kinetoplastidae* family, namely *Leishmania*, which is taxonomic to *Trypanosoma*, and identified various hit/lead compounds (Ndlovu et al., 2023; Zuma et al., 2023, 2022).

The clinical efficacy of NFT, an antibacterial medication used to treat urinary tract infections, is dependent on the elevated urine drug concentration that occurs during therapeutic administration, and as such, low blood drug concentrations are usually observed (Conklin, 1978). The pharmacological usefulness of NFT, a Biopharmaceutics Classification System class II item, is limited by its low water solubility and low plasma concentrations (Conklin, 1978; Teoh et al., 2020). Previously, structural modifications to nitrofurans led to considerable improvements in their physicochemical and pharmacokinetic properties, such as solubility, bioavailability, protein binding affinity, and even toxicity (Zuma et al., 2020). To improve the poor water solubility of NFT, hydrolytically and enzymatically stable hydrosoluble groups (Ndlovu et al., 2023) such as ethylene oxide oligomers were anchored to the α -N atom (Ndlovu et al., 2023). These oligomers are widely used in the pharmaceutical industry due to their good physical properties, including high water solubility (Spitzer et al., 2002). Additionally, they are

nontoxic (Thompson et al., 2008), nonimmunogenic, and resistant to biodegradation (Vadala et al., 2008). In addition to the oligomeric ethylene glycol (EG) moiety, other groups including pyrrolidone and propargyl were incorporated (Ndlovu et al., 2023).

Based on the above reports which suggest that some nitrofurans analogues may be used against AT, we evaluated the *in vitro* trypanocidal potency of NFT and its derivatives **2a-o** and discussed the observed structure-activity relationships. Additionally, we assessed the preliminary *in vivo* treatment efficacy of hit trypanocidal against the animal infective trypanosome *T. congolense* IL3000 in a rodent model.

2. Materials and methods

2.1. Test compounds

NFT (**1a**) and its derivatives **2a-o** (Table 1) were previously synthesized by Ndlovu et al. (2023). The test compounds were dissolved at a concentration of 10 mg/mL in 100 % dimethyl sulfoxide (DMSO) for *in vitro* assays and at a concentration of 100 mg/mL in 100 % DMSO for *in vivo* assays and then stored at $-4 \text{ }^{\circ}\text{C}$. For the *in vitro* assays, the test compounds were serially diluted with growth medium to 0.5 % DMSO. Notably, these serial dilutions were freshly prepared for each biological replicate. For the *in vivo* assays, the test compounds were diluted to 10 % DMSO with corn oil and 1 % DMSO with phosphate-buffered saline (PBS) for oral and intraperitoneal administration, respectively. Again, these treatments were freshly prepared daily.

2.2. *In silico* physicochemical and pharmacokinetic properties

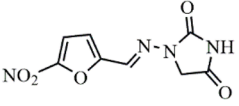
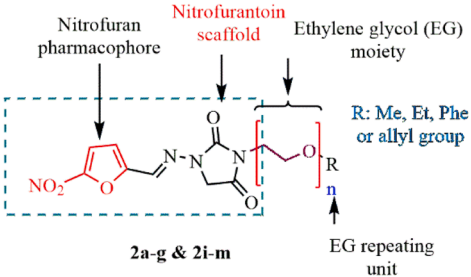
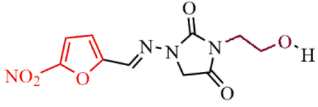
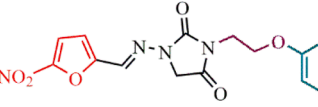
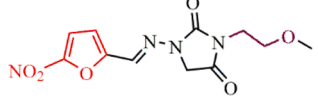
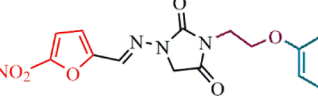
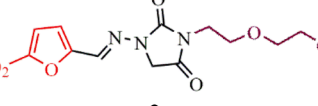
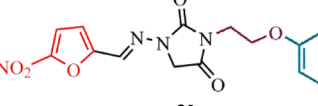
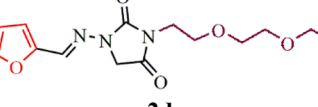
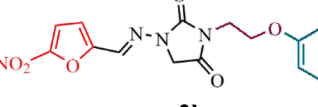
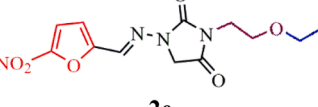
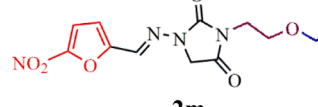
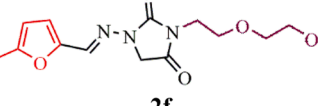
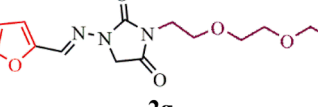
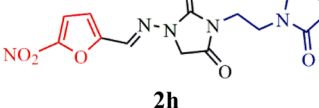
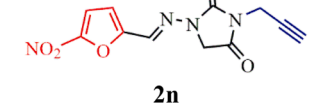
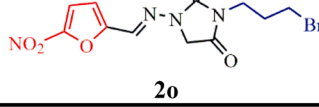
The physicochemical and pharmacokinetic properties of NFT (**1a**) and its derivatives **2a-o** (Appendix A) were computed using the SwissADME web tool (<http://www.swissadme.ch>).

2.3. *In vitro* cytotoxicity

The cytotoxicity of the synthesized test compounds was evaluated using Cell Counting Kit-8 (CCK-8; Dojindo Laboratories, Kumamoto, Japan) in a colorimetric assay (Ishiyama et al., 1997; Tominaga et al., 1999). Madin-Darby Bovine Kidney cells (MDBK; NBL-1; Japanese Collection of Research Bioresources cell bank, National Institute of Biomedical Innovation, Health and Nutrition) were cultured in Minimum Essential Medium Eagle (MEM; Sigma-Aldrich) with Earle's salts, L-glutamine, and sodium bicarbonate supplemented with 1 % penicillin-streptomycin (Thermo Fisher Scientific) and 10 % heat-inactivated fetal bovine serum (Thermo Fisher Scientific) at $37 \text{ }^{\circ}\text{C}$ (5 % CO_2).

Briefly, 96-well plates (Thermo Fisher Scientific) containing 50 μL of the cell suspension (1×10^5 cells/mL) and 50 μL of the test compound solution two times serially diluted at nine different concentrations (100–0.390625 $\mu\text{g}/\text{mL}$) were incubated at $37 \text{ }^{\circ}\text{C}$ (5 % CO_2) for 72 h. Then, the condition of the cells was observed with phase-contrast microscopy, and subsequently, 10 μL of the CCK-8 solution (Dojindo Laboratories, Kumamoto, Japan) was added, and the absorbance before (T_0) and after 4 h (T_4) of incubation was measured at 450 nm using a

Table 1
Synthesized oligomeric EG and other analogues of nitrofurantoin.

| EG-linked NFT analogues | | | | | |
|--------------------------------------------------------------------------------------------------------------------|---|-----------------------------------------------------------------------------------------------------------|--------------------------------------------------------------------------------------------|---|---------------------------|
|  <p>Nitrofurantoin (NFT) - 1a</p> | |  <p>2a-g & 2i-m</p> | | | |
| Compound | n | R | Compound | n | R |
|  2a | 1 | H |  2i | 1 | Phe |
|  2b | 1 | Me |  2j | 1 | 4-BrPhe |
|  2c | 2 | Me |  2k | 1 | 4-ClPhe |
|  2d | 3 | Me |  2l | 1 | 4-NO ₂ Ph e |
|  2e | 1 | Et |  2m | 1 | Allyl |
|  2f | 2 | Et | Other NFT analogues | | |
|  2g | 3 | Et |  2h | | |
| | | |  2n | | |
| | | |  2o | | |

GloMax-Multi Detection System plate reader (Promega) (Molefe et al., 2017; Munsimbwe et al., 2021; Narita et al., 2021). The experiments were conducted in triplicate. Data analysis for each biological replicate was performed using Microsoft Excel. The absorbance value at T_0 was subtracted from the absorbance value at T_4 , the mean absorbance was calculated, and the percentage cell viability was calculated by the following equation:

$$\text{Cell viability \%} = \frac{(\Delta \text{ Abs sample} - \Delta \text{ Abs blank})}{(\Delta \text{ Abs neg control} - \Delta \text{ Abs blank})} \times 100$$

The half maximum cytotoxic concentration (CC_{50}) for each test compound was calculated by non-linear regression (curve fit analysis) using GraphPad Prism version 8 software (GraphPad, Inc., San Diego, CA, USA) and represented as the mean \pm standard deviation (SD).

2.4. *In vitro* trypanocidal potency

The trypanocidal potency of the synthesized test compounds was evaluated using Cell-Titer Glo (Promega) in an ATP-based luciferase viability assay (Suganuma et al., 2014, 2017). Bloodstream forms of *T. b. gambiense* strain IL1922, *T. b. rhodesiense* strain IL1501, *T. b. brucei* strain GUTat3.1, *T. congolense* strain IL3000, *T. evansi* strain Tansui, and *T. equiperdum* strain IVM-t1 were cultured in Hirumi's Modified Iscove's Medium-9 (HMI-9) (Hirumi and Hirumi, 1991) at 37 °C and 5 % CO_2 (33 °C for *T. congolense* strain IL3000). HMI-9 consists of Iscove's Modified Dulbecco's Medium (DMEM; Sigma-Aldrich) supplemented with 1 % l-glutamine (Thermo Fisher Scientific), 1 % penicillin-streptomycin (Thermo Fisher Scientific), 0.1 mM bathocuproine (Sigma-Aldrich), 1 mM pyruvic acid sodium salt (Sigma-Aldrich), 1 mM hypoxanthine and 16 μ M thymidine (HT supplement; Thermo Fisher Scientific), 10 μ g/L insulin, 5.5 μ g/L transferrin and 6.7 ng/L sodium selenite (ITS-X; Thermo Fisher Scientific), 0.0001 % 2- β -mercaptoethanol (Sigma-Aldrich), 2 mM l-cysteine (Sigma-Aldrich), 60 mM HEPES (Sigma-Aldrich), 0.4 g/L bovine serum albumin (Sigma-Aldrich), and 20 % heat inactivated fetal bovine serum (Thermo Fisher Scientific). *T. b. gambiense* strain IL1922, *T. b. rhodesiense* strain IL1501, *T. b. brucei* strain GUTat3.1, *T. congolense* strain IL3000, and *T. evansi* strain Tansui were provided by Dr. Hirumi, while *T. equiperdum* strain IVM-t1 was established by Dr. Suganuma (Suganuma et al., 2016, 2017).

Briefly, Nunc MicroWell 96-well optical bottom plates (Thermo Fisher Scientific) containing 50 μ L of the bloodstream form of either *T. b. gambiense* strain IL1922, *T. b. rhodesiense* strain IL1501, *T. b. brucei* strain GUTat3.1 (2.5×10^3 cells/mL), *T. congolense* strain IL3000 (1×10^5 cells/mL), *T. evansi* strain Tansui, or *T. equiperdum* strain IVM-t1 (1×10^4 cells/mL) and 50 μ L of the test compound solution two times serially diluted at seven different concentrations (highest: 3.125 μ g/mL; lowest: 1.525 ng/mL) were incubated at 37 °C and 5 % CO_2 (33 °C for *T. congolense* strain IL3000) for 72 h. Then, the condition of the bloodstream-form trypanosomes was observed with phase-contrast microscopy, and subsequently, 25 μ L of the Cell-Titer Glo solution (Promega) was added, the plate was shaken for 2 min (500 shakes/min) using a MS3 basic plate shaker (IKA, Japan K.K., Osaka, Japan) to facilitate cell lysis and the release of intracellular ATP, whereupon the luminescence was measured at 450 nm using a GloMax-Multi Detection System plate reader (Promega) (Molefe et al., 2017; Munsimbwe et al., 2021; Narita et al., 2021; Suganuma et al., 2014). The experiments were conducted in triplicate. Data analysis for each biological replicate was performed using Microsoft Excel. The percentage cell viability was calculated as described in Section 2.3. The half maximum inhibitory concentration (IC_{50}) of each test compound was calculated by non-linear regression (curve fit analysis) using GraphPad Prism version 8 software (GraphPad, Inc., San Diego, CA, USA) and represented as the mean \pm standard deviation (SD). The selectivity index, which estimates the intrinsic activity of a test compound, was calculated by dividing the

trypanocidal potency (IC_{50}) of each test compound into its cytotoxicity (CC_{50}).

2.5. *In vivo* treatment efficacy

The *in vivo* animal experiment was carried out under approval of the Animal Ethics Committee of the Obihiro University of Agriculture and Veterinary Medicine (Approval No. 22–11) and performed as previously described (Molefe et al., 2017; Munsimbwe et al., 2021; Suganuma et al., 2022) while adhering to the European Community guidelines as accepted principles for the use of experimental animals. Healthy female 9-week-old BALB/cAJc1 mice (CLEA Japan, Inc., Tokyo, Japan) weighing 20–30 g each were housed in plastic cages at 25 ± 2 °C with 60 ± 10 % relative humidity under a 12-h light and dark cycle at the animal facility of the National Research Center for Protozoan Disease, Obihiro University of Agriculture and Veterinary Medicine. All mice had free access to normal food and water. The clinically significant *T. congolense* strain IL3000 was propagated in a mouse and used for further infection of other mice by intraperitoneal injection with 100 μ L of *T. congolense* strain IL3000 in phosphate-buffered saline, containing 10 % glucose at 1×10^4 cells/mL. Parasitemia was confirmed by microscopic observation. Mice were randomly assigned to three groups of two mice each as follows: group I served as positive control (infected and untreated), while group II (2k) and III (2l) mice were infected and treated with either 100 mg/kg/day of test compound 2k or 2l orally or 10 mg/kg/day of test compound 2k or 2l intraperitoneally. Treatment started four days post-infection and continued for seven successive days. These treatments were newly prepared each day using 10 % DMSO in corn oil for oral administration and 1 % DMSO in PBS for intraperitoneal administration. Parasitemia was assessed daily by wet smear with fresh blood collected from the tail vein. Additionally, a 1 μ L blood sample in 100 μ L of PSG was also collected daily and the number of trypanosomes present in a 1 000 times dilution was assessed using a Neubauer cell counting chamber (Watson Co., LTD, Tokyo, Japan). The *in vivo* treatment efficacy of 2k and 2l in this preliminary study did not justify any further *in vivo* animal experiments using more mice per group. The Kaplan-Meier method was used to generate survival curves and the differences between groups were analyzed using the log-rank test. All analyses were performed using GraphPad Prism version 8 software (GraphPad, Inc., San Diego, CA, USA).

3. Results and discussion

3.1. Predicted physicochemical and pharmacokinetic properties

Of all the physicochemical properties, lipophilicity is the most important; since it influences solubility, absorption from the gastrointestinal (GI) tract, membrane permeability, distribution via the blood by binding to plasma proteins, blood-brain barrier (BBB) permeation, as well as *in vivo* toxicological outcomes (Badiani, 2014). Poor water solubility is generally associated with high lipophilicity, while hydrophilic compounds generally show poor permeability, and thus, low absorption, which significantly influences bioavailability (Van De Waterbeemd and Gifford, 2003). Therefore, the early assessment of the physicochemical properties of test compounds during the drug discovery process is essential, and ultimately, reduces pharmacokinetics-related failures in the succeeding clinical phases (Hay et al., 2014). A summary of the physicochemical and pharmacokinetic properties of NFT (1a) and its analogues 2a–o can be found in Appendix A, Tables 2A–4A and Figs. 1A and 2A.

The partition coefficient of a molecule between octanol (lipophilic phase) and water (hydrophilic phase), or $\log P_{o/w}$, describes its lipophilicity and is an important component of Lipinski's "rule of five" which outlines physicochemical properties that support the drug-likeness of a compound (Lipinski et al., 1997). According to Lipinski's "rule of five", $\log P < 5$ increases the likelihood of absorption upon oral

administration (Lipinski et al., 1997). For validated hit and lead compounds intended for the treatment of infectious diseases, an ideal $\log P$ is between 1 and 3 (Goodwin et al., 2017; Katsuno et al., 2015). NFT (1a) and its analogues 2a-o have predicted $\log P$ values below 1, and thus, do not fall within the ideal 1–3 range (Appendix A, Table 2A). NFT (1a) and analogues 2a-h and 2l-m were predicted to be more hydrophilic ($-1.47 > \log P < -0.11$) since these compounds have negative $\log P$

values which indicate a higher affinity for the aqueous phase, while 2i-k and 2n-o have positive $\log P$ values ($0.07 < \log P < 0.97$) which denote a higher concentration in the lipid phase, meaning that these compounds are more lipophilic, and ultimately, have low water solubility which leads to variable oral absorption. It was noted that for derivatives 2c ($n = 2$; $\log P -1.24$) versus 2d ($n = 3$; $\log P -1.47$) and 2e ($n = 1$; $\log P -0.075$) versus 2g ($n = 3$; $\log P -0.97$), increased *n*-EG chain length led

Table 2

In vitro cytotoxicity and trypanocidal potency of NFT (1a) and its analogues (2a-2o).

| Compound | Cytotoxicity CC ₅₀ ± SD (µM) ^a | Trypanocidal potency IC ₅₀ ± SD (µM) ^a (SI) ^b | | | | | |
|------------------------------------|---------------------------------------------------------|--------------------------------------------------------------------------------------|-------------------------|-------------------------|-------------------------|---------------------------|-------------------------|
| | | MDBK | Tbg IL1922 | Tbr IL1501 | Tbb GuTat3.1 | Tc IL3000 | Tev Tansui |
| NFT | | | | | | | |
| 1a | 73.02 ± 36.15 | 1.85 ± 0.23 (39.47) | 1.69 ± 0.20 (43.21) | 1.51 ± 0.03 (48.36) | 0.42 ± 0.05 (173.9) | 1.67 ± 0.07 (43.72) | 1.45 ± 0.03 (50.36) |
| EG-linked NFT analogues | | | | | | | |
| 2a | 91.67 ± 28.81 | 0.62 ± 0.03 (147.9) | 0.65 ± 0.03 (141.0) | 0.62 ± 0.02 (147.9) | 0.36 ± 0.04 (254.6) | 1.15 ± 0.25 (79.71) | 0.84 ± 0.16 (109.1) |
| 2b | 45.81 ± 14.28 | 1.16 ± 0.02 (39.49) | 1.21 ± 0.02 (37.86) | 1.18 ± 0.05 (38.82) | 0.75 ± 0.07 (61.08) | 3.00 ± 0.55 (15.27) | 2.33 ± 0.06 (19.66) |
| 2c | 77.32 ± 10.05 | 1.41 ± 0.23 (54.84) | 1.80 ± 0.18 (42.96) | 1.20 ± 0.01 (64.43) | 0.99 ± 0.11 (78.10) | 3.67 ± 0.42 (21.07) | 2.44 ± 0.37 (31.69) |
| 2d | 78.52 ± 14.41 | 0.94 ± 0.04 (83.53) | 1.12 ± 0.08 (70.11) | 0.95 ± 0.04 (82.65) | 0.72 ± 0.10 (109.1) | 2.91 ± 0.66 (26.98) | 1.98 ± 0.20 (39.66) |
| 2e | 48.64 ± 10.35 | 1.91 ± 0.44 (25.47) | 2.20 ± 0 (22.11) | 1.51 ± 0.09 (32.21) | 0.94 ± 0.18 (51.74) | 5.06 ± 0.06 (9.61) | 4.30 ± 0.95 (11.31) |
| 2f | 50.07 ± 11.32 | 1.12 ± 0.13 (44.71) | 1.34 ± 0.13 (37.37) | 1.05 ± 0.03 (47.69) | 0.68 ± 0.07 (73.63) | 4.60 ± 0.17 (10.88) | 3.46 ± 0.89 (14.47) |
| 2g | 66.72 ± 2.46 | 1.54 ± 0.3 (43.32) | 1.79 ± 0.04 (37.27) | 1.55 ± 0.18 (43.05) | 0.95 ± 0.19 (70.23) | 4.25 ± 0.52 (15.70) | 3.38 ± 0.70 (19.74) |
| 2i | 30.34 ± 1.90 | 1.63 ± 0.52 (18.61) | 1.88 ± 0.27 (16.14) | 1.18 ± 0.20 (25.71) | 0.16 ± 0.02 (189.6) | 8.32 ± 0.32 (3.65) | 8.29 ± 0.24 (3.66) |
| 2j | >228.64 | 0.38 ± 0.09 (>601.7) | 0.45 ± 0.01 (>508.1) | 0.32 ± 0.07 (>714.5) | 0.06 ± 0.01 (>3811) | 4.31 ± 0.51 (>53.05) | 3.21 ± 0.69 (>71.23) |
| 2k | >254.61 | 0.23 ± 0.05 (>1107) | 0.30 ± 0.07 (>848.7) | 0.20 ± 0.03 (>1273) | 0.04 ± 0.01 (>6365) | 3.46 ± 0.34 (>73.59) | 2.32 ± 0.58 (>109.8) |
| 2l | >247.95 | 0.19 ± 0.04 (>1305) | 0.22 ± 0.01 (>1127) | 0.12 ± 0.01 (>2066) | 0.06 ± 0.02 (>4133) | 8.09 ± 0.49 (>30.65) | 2.03 ± 1.35 (>122.1) |
| 2m | 31.28 ± 7.04 | 1.87 ± 0.44 (16.73) | 2.15 ± 0.02 (14.55) | 1.53 ± 0.52 (20.44) | 0.71 ± 0.07 (44.06) | 9.17 ± 1.13 (3.41) | 7.79 ± 1.97 (4.02) |
| Other NFT analogues | | | | | | | |
| 2h | 49.53 ± 6.21 | 0.51 ± 0.03 (97.12) | 0.61 ± 0.04 (81.20) | 0.51 ± 0.02 (97.12) | 0.72 ± 0.06 (68.79) | 1.03 ± 0.07 (48.09) | 0.88 ± 0.16 (56.28) |
| 2n | >362.04 | 4.33 ± 0.68 (>83.61) | 5.04 ± 0.58 (>71.83) | 3.40 ± 0.80 (>106.5) | 0.74 ± 0.16 (>489.2) | 21.87 ± 2.5 (16.55) | 14.87 ± 5.5 (>24.35) |
| 2o | 33.83 ± 0.31 | 0.52 ± 0.02 (65.06) | 0.54 ± 0.04 (62.65) | 0.50 ± 0.02 (67.66) | 0.32 ± 0.02 (105.7) | 1.02 ± 0.1 (33.17) | 0.86 ± 0.22 (39.34) |
| Reference drugs^d | | | | | | | |
| Eflornithine | – | 16.13 ± 2.93 | 38.56 ± 9.88 | 36.66 ± 12.87 | 45.99 ± 17.07 | 57.21 ± 17.56 | – |
| Nifurtimox | – | 1.06 ± 0.22 | 4.66 ± 19.70 | 4.58 ± 2.38 | 4.35 ± 1.59 | 2.62 ± 1.40 | – |
| Pentamidine | – | 0.33 ± 0.05 | 0.041 ± 0.0023 | 0.014 ± 0.0031 | 0.029 ± 0.0062 | 0.00097 ± 0.00019 | 0.0013 ± 0.0003 |
| Suramin | – | 7.17 ± 0.87 | 0.066 ± 0.0052 | 0.064 ± 0.0018 | 0.076 ± 0.011 | 0.38 ± 0.058 ^c | 0.038 ± 0.014 |
| Diminazene aceturate | – | – | – | – | 0.109 ± 0.026 | – | 0.011 ± 0.0029 |

^a Half maximal cytotoxic concentration (CC₅₀, µM) represented as the mean ± standard deviation (SD), three biological replicates.

^b Half maximal inhibitory concentration (IC₅₀, µM) represented as the mean ± standard deviation (SD), three biological replicates.

^c Selectivity index (SI): CC₅₀ (µM) / IC₅₀ (µM).

^d IC₅₀ values obtained from literature (Munsimbwe et al., 2021; Saganuma et al., 2014, 2017) NFT: nitrofurantoin; MDBK: Madin-Darby bovine kidney cells; Tbg IL1922: *Trypanosoma brucei gambiense* strain IL1922; Tbr IL1501: *Trypanosoma brucei rhodesiense* strain IL1501; Tbb GuTat3.1: *Trypanosoma brucei* strain GuTat3.1; Tc IL3000: *Trypanosoma congolense* strain IL3000; Tev Tansui: *Trypanosoma evansi* strain Tansui; Teq IVM-t1: *Trypanosoma equiperdum* strain IVM-t1; qualifies as hit compound if IC₅₀ ≤ 10 µM and SI ≥ 10 (Nwaka and Hudson, 2006) The parent drug NFT has a well-known safety profile which allowed the establishment of an initial reference for *in vitro* toxicity. NFT (1a) previously showed low cytotoxic activities (CC₅₀ > 100 µM) towards HEK-293 (Zuma et al., 2022), THP-1 and Vero cells (Ndlovu et al., 2023; Zuma et al., 2023), as did derivatives 2b, 2i-k and 2m-n, except 2o which was mild/moderately toxic (CC₅₀ 61.99 µM) (Ndlovu et al., 2023). Towards MDBK cells, derivatives 2j-l and 2n also showed low basal toxicity (CC₅₀ ≥ 100 µM) (Adewusi et al., 2013; Fu et al., 2014), while 2a, 2c-d and 2f-g were weakly toxic (50 µM ≤ CC₅₀ ≤ 100 µM) (Liu et al., 2017) and 2b, 2e, 2h-i, 2m and 2o were mild/moderately toxic (10 µM ≤ CC₅₀ ≤ 50 µM) (Gill and Malhotra, 1963; Liu et al., 2017). Despite being weakly to mild/moderately toxic towards MDBK cells, these derivatives were 10 to 100-fold selective in their trypanocidal action. The phenoxy derivative 2i (CC₅₀ 30.34 µM) and nucleophilic allyl analogue 2m (CC₅₀ 31.28 µM) and 3-bromopropyl analogue 2o (CC₅₀ 33.83 µM) were the most toxic of all test compounds. The aforementioned derivatization with these moieties was thus detrimental to the safety of NFT.

to increased hydrophilicity, which is to be expected since oligomeric EG is highly water soluble (Spitzer et al., 2002). For the halogenated phenoxy derivatives **2j** (-Br; $\log P$ 0.97), **2k** (-Cl; $\log P$ 0.85), and **2l** (-NO₂; $\log P$ -0.11), lipophilicity increased with decreased electron negativity (EN). All derivatives were expected to have high GI absorption and oral bioavailability (except **2l** and **2d** due to their $TPSA \geq 140$ and $RB \geq 10$) (Veber et al., 2002) but none of these analogues were foreseen to cross the BBB (Appendix A, Table 3A). All compounds complied with Lipinski's rules and were considered drug-like (Appendix A, Table 4A), except **2c-d** and **2f-h** which violate one of Lipinski's rules (N or $O < 10$). Notably, Lipinski's rules are only used to prioritize hits and should not be used as definitive selection criteria.

3.2. Pharmacology

3.2.1. In vitro cytotoxicity

Toxicity often hinders the drug development process and adds to its high cost (Guengerich, 2011); therefore, determination of the preliminary safety of a drug candidate is vital. General cytotoxicity of NFT

(**1a**) and its analogues **2a-o** towards MDBK cells are summarized in Table 2.

It was observed that as n -EG chain length increased and lipophilicity decreased, toxicity also decreased (Fig. 3A); for example, **2b** ($n = 1$; CC_{50} 45.81 μ M) > **2c** ($n = 2$; CC_{50} 77.32 μ M) > **2d** ($n = 3$; CC_{50} 78.52 μ M) and **2e** ($n = 1$; CC_{50} 48.64 μ M) > **2f** ($n = 2$; CC_{50} 50.07 μ M) > **2g** ($n = 3$; CC_{50} 66.72 μ M). Furthermore, derivative **2a** containing a terminal hydroxy group was weakly toxic (CC_{50} 91.67 μ M), while the more lipophilic **2b**, **2e**, and **2m** containing terminal methoxy, ethoxy, and allyl groups, respectively, were mild/moderately toxic (31.28μ M > CC_{50} < 48.64 μ M). Comparison of **2i** (CC_{50} 30.34 μ M) to its phenoxy counterparts **2j** (4-BrPhe; CC_{50} >228.64 μ M), **2k** (4-ClPhe; CC_{50} >254.61 μ M) and **2l** (4-NO₂Phe; CC_{50} >247.95 μ M) showed a ten-fold decrease in toxicity from mild/moderately toxic to non-toxic, and as electron negativity (EN) increased, lipophilicity decreased, and toxicity also decreased (Fig. 3A). This corroborates a previous finding that higher lipophilicity is often associated with higher toxicity (Van De Waterbeemd and Gifford, 2003).

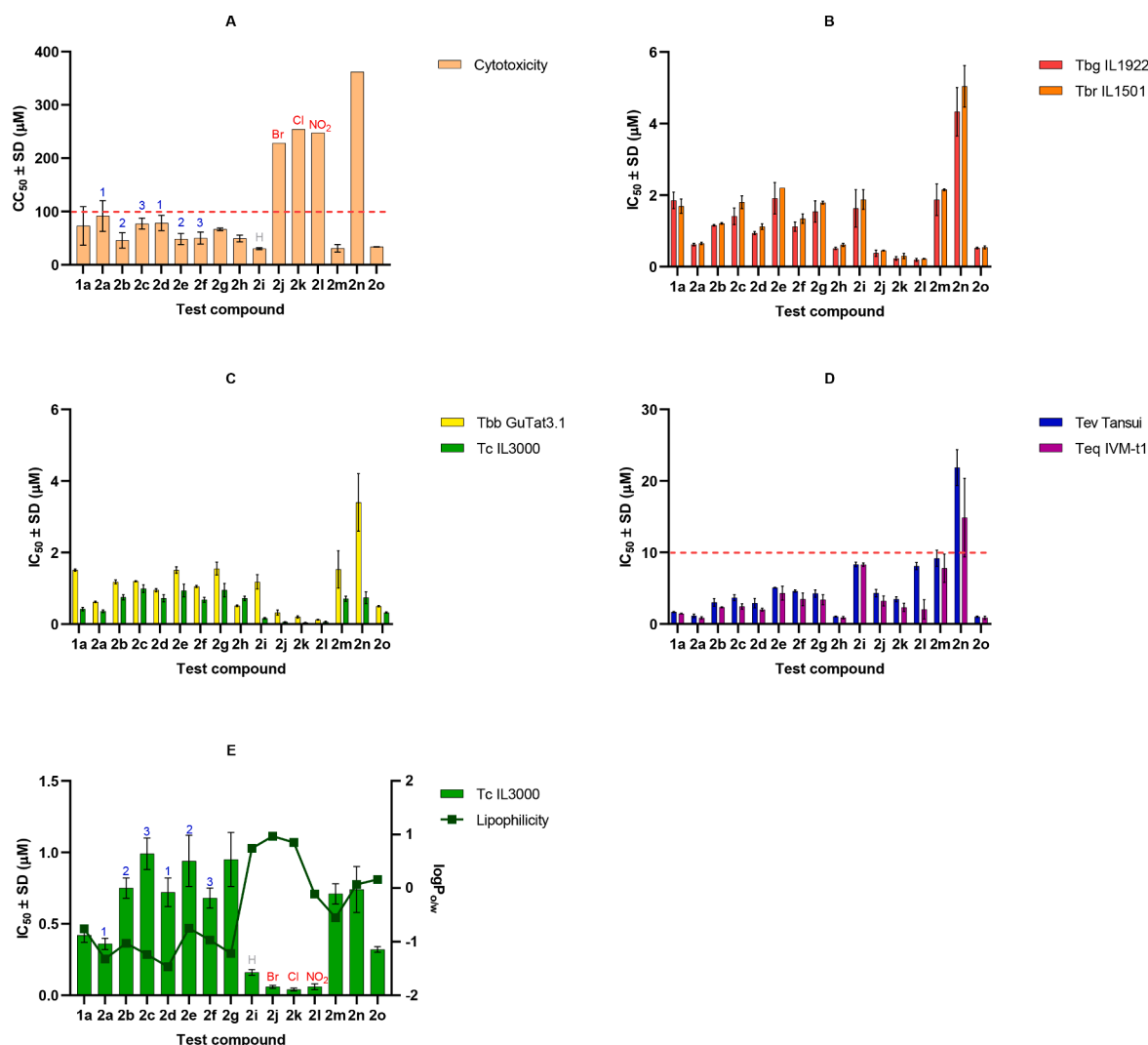


Fig. 3. A Cytotoxicity ($CC_{50} \pm SD$, μ M) towards Madin-Darby bovine kidney (MDBK) cells. Low cytotoxicity above red dashed line. n -EG chain length indicated in blue, neutral group (H) indicated in grey, and electron withdrawing groups in order of increasing strength (Br, Cl, NO₂) indicated in red. Comparison of trypanocidal activities ($IC_{50} \pm SD$, μ M) against B tsetse-transmitted human infective trypanomastigotes of *T. b. gambiense* strain IL1922 and *T. b. rhodesiense* strain IL1501; C tsetse-transmitted animal infective trypanomastigotes of *T. b. brucei* GuTat3.1 strain GuTat3.1 and *T. congolense* strain IL3000; D non-tsetse transmitted animal infective trypanomastigotes of *T. evansi* strain Tansui, and *T. equiperdum* strain IVM-t1. Hit trypanocidal activity below red dashed line. E Comparison of trypanocidal activity against *T. congolense* strain IL3000 trypanomastigotes and lipophilicity ($\log P_{o/w}$). n -EG chain length indicated in blue, neutral group (H) indicated in grey, and electron withdrawing groups in order of increasing strength (Br, Cl, NO₂) indicated in red.

3.2.2. *In vitro* trypanocidal potency and hit/lead identification

Numerous challenges must be overcome to develop new anti-trypanosomal agents. This led experts in the field of drug discovery to establish various strategies to fast-track the lengthy drug discovery process. At the basic research stage, established hit and lead criteria for human AT require that an IC_{50} value must be less than $10\ \mu\text{M}$ and the selectivity index greater than 10 for the bloodstream form trypomastigotes of *T. b. brucei* species (Nwaka and Hudson, 2006). A lead, on the other hand, should show a 10 to 20-fold increase in activity over the hit and be active against bloodstream form trypomastigotes of *T. b. gambiense* and/or *T. b. rhodesiense* (Nwaka and Hudson, 2006).

The trypanocidal potency of NFT (**1a**) and its analogues **2a-o** against axenically cultured bloodstream form trypomastigotes of *T. b. gambiense* strain IL1922, *T. b. rhodesiense* strain IL1501, *T. b. brucei* strain GUTat3.1, *T. congolense* strain IL3000, *T. evansi* strain Tansui, and *T. equiperdum* strain IVM-t1 are summarized in Table 2.

Based on the aforementioned criteria, analogues **2a-o** generally showed hit trypanocidal activity against the six species of human or animal infective trypanosomes (Fig. 3B–D), with the best activity observed against *T. congolense* strain IL3000 (Fig. 3E). Derivatives **2d**, **2i**, **2m** showed weak activity against ($IC_{50} > 10\ \mu\text{M}$) and/or selectivity ($SI < 10$) for *T. evansi* strain Tansui and/or *T. equiperdum* strain IVM-t1. Compared to *T. congolense* strain IL3000, trypanocidal activities decreased almost 4-fold across the board against the phylogenetically related *T. brucei* complex organisms as well as *T. evansi* strain Tansui and/or *T. equiperdum* strain IVM-t1 parasites. The best activity against and selectivity for *T. congolense* strain IL3000 was shown by the arylated derivative **2k** (4-ClPhe: IC_{50} $0.04\ \mu\text{M}$), closely followed by **2l** (4-NO₂Phe: IC_{50} $0.06\ \mu\text{M}$) and **2j** (4-BrPhe: IC_{50} $0.06\ \mu\text{M}$). Notably, derivatives **2j-l** showed 2 to 3-fold better activity against *T. congolense* strain IL3000 than the commonly used veterinary antitrypanosomal agent diamizene acetate (IC_{50} $0.109\ \mu\text{M}$) (Suganuma et al., 2014). The nitro phenoxy analogue **2l** showed the best activity against *T. brucei* complex organisms ($0.12\ \mu\text{M} > IC_{50} < 0.22\ \mu\text{M}$), while the ethoxy triethylene glycol (TEG) analogue **2g** ($n = 3$; $R = \text{Et}$) showed the best activity against *T. evansi* (IC_{50} $4.25\ \mu\text{M}$) and *T. equiperdum* (IC_{50} $3.38\ \mu\text{M}$).

3.2.3. Structure-activity relationships

Structure-activity relationships (SAR) will be discussed based on trypanocidal activity against *T. congolense* strain IL3000, since analogues **2a-o** showed the best activity against the said trypanosome. The variation of two parameters, namely predicted lipophilicity and electronic effect were considered.

3.2.3.1. Alkoxy-EG analogues. The variation of lipophilicity modulated by *n*-EG chain length was considered for analogues **2a-g**. For the methylated derivatives **2b** ($n = 1$; $\log P -1.03$; IC_{50} $0.75\ \mu\text{M}$), **2c** ($n = 2$; $\log P -1.24$; IC_{50} $0.99\ \mu\text{M}$) and **2d** ($n = 3$; $\log P -1.47$; IC_{50} $0.72\ \mu\text{M}$), as well as the ethylated derivatives **2e** ($n = 1$; $\log P -0.75$; IC_{50} $0.94\ \mu\text{M}$), **2f** ($n = 2$; $\log P -0.97$; IC_{50} $0.68\ \mu\text{M}$) and **2g** ($n = 3$; $\log P -1.22$; IC_{50} $0.95\ \mu\text{M}$), as *n*-EG chain length increased, lipophilicity decreased (as expected since oligomeric EG is highly water soluble (Spitzer et al., 2002)).

Activity increased from $n = 1$ (**2b** and **2e**) to $n = 2$ (**2c** and **2f**) but then decreased again from $n = 2$ to $n = 3$ (**2d** and **2g**) giving a similar IC_{50} value as $n = 1$ (Fig. 3E).

We also examined the variation of lipophilicity modulated by the terminal R group. For a fixed *n*-EG chain length and varying terminal R group (either methyl (Me) or ethyl (Et)), as lipophilicity increased, trypanocidal activity decreased exemplified by **2b** ($R = \text{Me}$; $\log P -1.03$; IC_{50} $0.75\ \mu\text{M}$) versus **2e** ($R = \text{Et}$; $\log P -0.75$; IC_{50} $0.94\ \mu\text{M}$) and **2d** ($R = \text{Me}$; $\log P -1.47$; IC_{50} $0.72\ \mu\text{M}$) versus **2g** ($R = \text{Et}$; $\log P -1.22$; IC_{50} $0.95\ \mu\text{M}$). Again $n = 2$ (**2c** and **2f**) was an exemption, and increased lipophilicity led to increased trypanocidal activity against *T. congolense* strain IL3000. The selectivity of test compounds for the trypanosomes over the mammalian cells generally improved as *n*-EG increased and lipophilicity decreased, while for a fixed *n*-EG chain length and varying terminal R group the more lipophilic ethyl group, led to decreased selectivity. Thus, a zig-zag pattern was observed for derivatives **2b-g**. It seems as though not only *n*-EG chain length but also the terminal R group influence lipophilicity, and consequently, the *in vitro* trypanocidal potency. A summary of SAR for the oligomeric EG analogues of NFT is depicted in Fig. 4.

3.2.3.2. Phenoxy analogues. Additionally, lipophilicity was modulated by electron negativity. The electron negativity (EN) among arylated analogues **2i-l** increased in the order: **2i** ($R = \text{Phe}$), **2j** (4-BrPhe), **2k** (4-ClPhe) and **2l** (4-NO₂Phe). These analogues showed decreased lipophilicity, and increased trypanocidal activity, albeit slight ($0.04\ \mu\text{M} > IC_{50} < 0.06\ \mu\text{M}$) (Fig. 3C and E). Notably, the halogenated phenoxy derivative **2k** displayed the best trypanocidal activity overall (IC_{50} $0.04\ \mu\text{M}$; $SI > 6365$). The presence of an electron-withdrawing group (EWG) such as bromine (**2j**), chlorine (**2k**) or nitro (**2l**) on the phenoxy ring, was shown to increase potency when compared to the neutral analogue **2i** (which showed the worst trypanocidal activity of the arylated derivatives, and interestingly, the greatest cytotoxicity) (Fig. 4). The most electron negative nitrophenoxy analogue **2l** (IC_{50} $0.06\ \mu\text{M}$; $SI > 4133$) showed similar trypanocidal activity to the least electron negative bromophenoxy **2j** (IC_{50} $0.06\ \mu\text{M}$; $SI > 3811$); however, **2l** had greater selectivity for the trypanosomes than the mammalian cells compared to **2j**. A similar trend was observed by other researchers (Munsimbwe et al., 2021; Ndlovu et al., 2023), who previously found that the anti-trypanosomal activities of analogues bearing EWGs were stronger than that of the neutral ones. Other studies have also reported the influence of the electronic effect on *in vitro* trypanocidal potency (Cuevas-Hernández et al., 2016; Salas et al., 2011; Vera et al., 2017). Hence, the appendage of a phenoxy group bearing an EWG to NFT through the oligomeric EG-linker, resulted in increased lipophilicity compared to the parent drug NFT, and altogether enhanced trypanocidal potency.

3.2.3.3. Other analogues. Derivative **2m** ($n = 1$; IC_{50} $0.71\ \mu\text{M}$) which contains an electron donating allyl, experienced a loss of trypanocidal activity when compared to its unsubstituted counterpart **2a** ($n = 1$; $R = \text{H}$; IC_{50} $0.36\ \mu\text{M}$). Exchange of the hydroxy group of **2a** with an electron withdrawing pyrrolidone ring resulted in derivative **2h** (IC_{50} $0.72\ \mu\text{M}$),

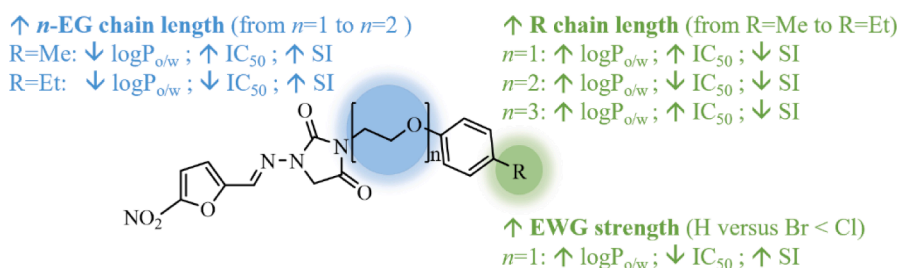


Fig. 4. Summary of structure-activity relationships. ↑: increased; ↓: decreased; $\log P_{o/w}$: log of partition coefficient of solute between octanol and water, indicator of lipophilicity; IC_{50} : half maximum inhibitory concentration; SI : selectivity index; EG: ethylene glycol; EWG: electron withdrawing groups; Me: methyl; Et: ethyl.

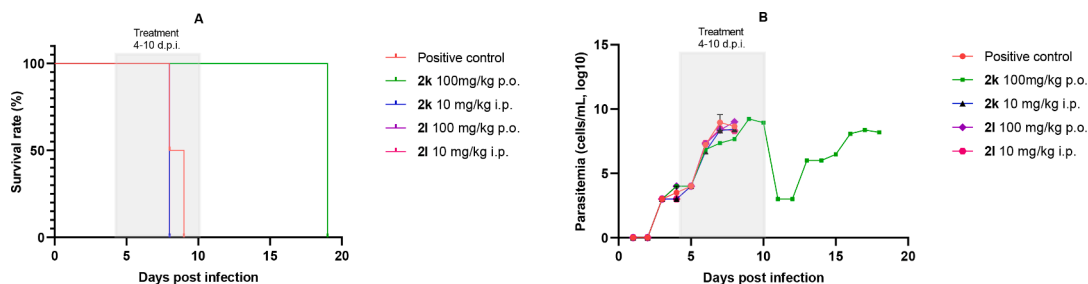


Fig. 5. *In vivo* evaluation of preliminary treatment efficacy of selected oligomeric EG-tethered nitrofurantoin derivatives. A Survival rate (%) and B parasitemia (cells/mL, log₁₀) of *T. congolense* strain IL3000 infected BALB/c mice left untreated (positive control), or treated with either 100 mg/kg of 2k or 2l orally or 10 mg/kg of 2k or 2l intraperitoneally from 4 days post infection. The survival rates of the treated mice were not significantly different from those of the untreated mice (*P*-value 0.34, log-rank test). *P*-values < 0.05 were considered statistically different. d.p.i.: days post-infection; p.o.: *per os*; i.p. intraperitoneal.

while the nucleophilic substitution at the terminal N-position of NFT with an electron donating propargyl group gave **2n** (IC₅₀ 0.74 μM). Both **2h** and **2n** analogues displayed an almost 2-fold decrease in potency when compared to the parent drug NFT. On the contrary, the N-nucleophilic substitution of NFT with 1,3-dibromopropane afforded the 3-bromopropyl analogue **2o** (IC₅₀ 0.0.32 μM) that is endowed with a slight increase in trypanocidal potency compared to NFT, presumably due to the electron withdrawing feature of the bromo group.

3.3. *In vivo* treatment efficacy

It was previously reported that a 100 % survival and cure (complete clearance of parasite without relapse) of *T. congolense* strain IL3000 infected BALB/c mice were achieved with a minimum dose of 30 mg/kg nitrofurantoin per day for seven days (Suganuma et al., 2022). While selected N-alkyl substituted NFT analogues showed no such treatment efficacy since these derivatives were insoluble in the *in vivo* testing medium (Munsimbwe et al., 2021). These results indicated that NFT analogues with high hydrophilicity were required for *in vivo* assessment to determine whether they are promising leads for developing trypanocidal drugs. To improve the poor water solubility of these NFT analogues, hydrolytically and enzymatically stable hydrosoluble groups, such as oligomeric EG were anchored to the α-N atom (Ndlovu et al., 2023).

Thus, the EG-anchored NFT analogues **2k** and **2l** were evaluated to determine their *in vivo* treatment efficacy based on their promising *in vitro* trypanocidal potency as well as drug-like properties (discussed in Sections 3.1. and 3.2.1-3.2.2., respectively). In this preliminary animal study, *T. congolense* strain IL3000 infected BALB/c mice were treated with either 100 mg/kg of test compound **2l** orally or 10 mg/kg of test compound **2k** or **2l** intraperitoneally, and all died within 9 dp.i. due to high parasitemia, similar to the infected but untreated control mice (Fig. 5). While the mouse treated with 100 mg/kg of test compound **2k** orally survived until 18 dp.i. and succumbed thereafter also due to high parasitemia (Fig. 5). Notably, parasitemia did briefly decrease on 11 and 12 dp.i. upon completion of treatment with 100 mg/kg of test compound **2k** orally, but no parasite clearance was achieved (Fig. 5B). Statistical analyses revealed that the survival rates of the treated mice were not significantly different from those of the untreated mice. Indeed, none of the mice survived until the end of the experiment period. Consequently, no mentionable *in vivo* treatment efficacy was observed against *T. congolense* strain IL3000 infected BALB/c mice, after oral or intraperitoneal administration of the test compounds since no cure (complete clearance of parasite without relapse) or survival was achieved. These preliminary results did not warrant any further *in vivo* animal studies using more mice per group.

As therapeutic behavior is modulated by pharmacokinetic and pharmacodynamic properties, it does not automatically mean that more potent drug candidates (such as analogues **2k** and **2l** compared to the parent drug NFT) will have greater clinical efficacy (Waldman, 2002).

Analogues **2k** and **2l** were thought to be orally bioavailable based on Lipinski's "rule of five"; however, oral bioavailability problems may be assumed based on these analogues' low lipophilicity (log*P* < 1) which, *in vivo*, leads to low absorption, a low volume of distribution, and ultimately, low bioavailability (Stocks, 2013). Indeed, poor oral bioavailability is often associated with incomplete absorption due to very slow and/or incomplete dissolution of the drug in the GI tract, incomplete absorption due to poor permeability of the drug through the intestinal epithelia, and/or biotransformation of the drug during its first passage through the liver (Raaflaub, 1980). Additionally, the test compounds had low solubility in the *in vivo* testing medium (either corn oil or PBS for oral or intraperitoneal administration, respectively), and formed quickly separating suspensions which hindered uniform dosing, and as such, limited the pharmacological usefulness of the investigated oligomeric EG-tethered NFT derivatives.

4. Conclusions

Many nitroheterocyclic drugs or compounds, including nitrofurantoin, showed, in addition to their clinical use as antibiotics, anti-parasitic activities. Thus, the current study was conducted to evaluate the *in vitro* trypanocidal potency, and ultimately, *in vivo* treatment efficacy of previously synthesized antileishmanial active oligomeric EG-tethered analogues of nitrofurantoin against an array of human and animal trypanosome species. The trypanocidal potency of analogues **2a-o** varied among the trypanosome species; however, *T. congolense* strain IL3000 was more susceptible to nitrofurantoin and its analogues than the other trypanosomes. The arylated derivatives **2j**, **2k**, and **2l** showed the best trypanocidal activity against *T. congolense* strain IL3000 in the nanomolar range with low toxicity against mammalian cells. Analogues **2a-o** had comparatively modest trypanocidal activities against, the human infective *T. b. gambiense* strain IL1922 and *T. b. rhodesiense* strain IL1501, as well as the animal infective *T. b. brucei* strain GuTat3.1, *T. evansi* strain Tansui, and *T. equiperdum* strain IVM-t1 in the sub- to micromolar ranges. Although the phenoxy derivatives **2k** and **2l** showed strong *in vitro* trypanocidal potency, no *in vivo* treatment efficacy was observed against *T. congolense* strain IL3000 infected BALB/c mice during a preliminary animal study. The inability of **2k** and **2l** to clear the parasites is probably due to their low solubility in the *in vivo* testing medium. Future work on oligomeric EG derivatives of NFT will focus on the investigation of novel analogues with improved physicochemical properties to achieve both solubility and membrane permeability to effectively treat *Trypanosoma* infections in animals and/or humans.

Funding

This work was supported by the Japan Society for the Promotion of Science (JSPS), KAKENHI grant number 16K18793 [Grants-in-Aid for Young Scientists (B)], grant number 148781 [NRF-JSPS Bilateral Joint Research Program], and Ohyama Health Foundation, Inc. The funders

had no role in the study design, data collection and interpretation, nor the decision to submit the work for publication.

Supplementary Information

The following supporting information can be found in Appendix A: names and structures of test compounds, the predicted physicochemical and pharmacokinetic properties of the test compounds.

CRedit authorship contribution statement

Helena D. Janse van Rensburg: Data curation, Formal analysis, Investigation, Writing – original draft, Writing – review & editing. **David D. N'Da:** Conceptualization, Data curation, Formal analysis, Funding acquisition, Investigation, Methodology, Project administration, Resources, Supervision, Writing – review & editing. **Keisuke Suganuma:** Conceptualization, Data curation, Formal analysis, Funding acquisition, Investigation, Methodology, Project administration, Resources, Software, Supervision, Validation, Writing – review & editing.

Declaration of Competing Interest

The authors have no relevant financial or non-financial interests to disclose.

Data availability

Data will be made available on request.

Acknowledgments

The authors would like to thank the Japan Society for the Promotion of Science (JSPS) and Ohyama Health Foundation, Inc. for providing financial assistance.

Supplementary materials

Supplementary material associated with this article can be found, in the online version, at [doi:10.1016/j.ejps.2023.106668](https://doi.org/10.1016/j.ejps.2023.106668).

References

- Adewusi, E.A., Steenkamp, P., Fouche, G., Steenkamp, V., 2013. Isolation of cycloeucaenol from *Boophone disticha* and evaluation of its cytotoxicity. *Nat. Prod. Commun.* 8, 1213–1216.
- Badiani, A., 2014. History of psychopharmacology. In: Stolerman, I., Price, L. (Eds.), *Encyclopedia of Psychopharmacology*. Springer.
- Barr, S.C., Saunders, A.B., Sykes, J.E., 2014. Trypanosomiasis, Canine and Feline Infectious Diseases. Elsevier, pp. 760–770.
- Bendford, D., Ceccatelli, S., Cottrill, B., DiNovi, M., Dogliotti, E., Lutz, E., 2015. Scientific Opinion on nitrofurans and their metabolites in food. *EFSA J.* 13, 4140.
- Blass, B.E., 2015. Case Studies in Drug discovery, Basic principles of Drug Discovery and Development. Elsevier, pp. 511–512.
- Blowey, R., Weaver, A.D., 2011. Infectious diseases, *Color Atlas of Diseases and Disorders of Cattle E-Book*. Elsevier, pp. 238–239.
- Borges, A.S., Mair, T., Pasval, I., Saulez, M.N., Tennent-Brown, B.S., van Eps, A.W., 2014. Emergency diseases outside the continental United States. In: Orsini, J.A., Divers, T. J. (Eds.), *Equine Emergencies*. Elsevier, pp. 656–686.
- Cayla, M., Rojas, F., Silvester, E., Venter, F., Matthews, K.R., 2019. African trypanosomes. *Parasit. Vect.* 12, 190.
- Chitanga, S., Marcotty, T., Namangala, B., Van den Bossche, P., Van Den Abbeele, J., Delepaux, V., 2011. High prevalence of drug resistance in animal trypanosomes without a history of drug exposure. *PLoS Negl. Trop. Dis.* 5, e1454.
- Chong, C.R., Sullivan, D.J., 2007. New uses for old drugs. *Nature* 448, 645–646.
- Conklin, J.D., 1978. The pharmacokinetics of nitrofurantoin and its related bioavailability. *Antibiot. Chemother.* (1971) 25, 233–252.
- Coustou, V., Guegan, F., Plazolles, N., Baltz, T., 2010. Complete *in vitro* life cycle of *Trypanosoma congolense*: development of genetic tools. *PLoS Negl. Trop. Dis.* 4, e618.
- Cuevas-Hernández, R.I., Correa-Basurto, J., Flores-Sandoval, C.A., Padilla-Martínez, I.I., Nogueada-Torres, B., Villa-Tanaca, M.d.L., Tamay-Cach, F., Nolasco-Fidencio, J.J., Trujillo-Ferrara, J.G., 2016. Fluorine-containing benzothiazole as a novel trypanocidal agent: design, *in silico* study, synthesis and activity evaluation. *Med. Chem. Res.* 25, 211–224.
- Deeks, E.D., 2019. Fexinidazole: first global approval. *Drug.* 79, 215–220.
- Desquesnes, M., Gonzatti, M., Sazmand, A., Thévenon, S., Bossard, G., Boulangé, A., Gimonneau, G., Truc, P., Herder, S., Ravel, S., 2022. A review on the diagnosis of animal trypanosomoses. *Parasit. Vect.* 15, 64.
- Doan, T.L., Pollastri, M., Walters, M.A., Georg, G.I., 2011. The future of drug repositioning: old drugs, new opportunities. In: Macor, J.E. (Ed.), *Annual Reports in Medicinal Chemistry*. Elsevier, pp. 385–401.
- Fu, J., Chen, H., Soroka, D.N., Warin, R.F., Sang, S., 2014. Cysteine-conjugated metabolites of ginger components, shogaols, induce apoptosis through oxidative stress-mediated p53 pathway in human colon cancer cells. *J. Agric. Food Chem.* 62, 4632–4642.
- Gallardo-Garrido, C., Cho, Y., Cortés-Rios, J., Vasquez, D., Pessoa-Mahana, C.D., Araya-Maturana, R., Pessoa-Mahana, H., Faundez, M., 2020. Nitrofurans beyond redox cycling: evidence of Nitroreduction-independent cytotoxicity mechanism. *Toxicol. Appl. Pharmacol.* 401, 115104.
- Gill, B., Malhotra, M., 1963. Prophylactic activity of suramin complexes in 'Surra' (*Trypanosoma evansi*). *Nature* 200, 285–286.
- Giordani, F., Morrison, L.J., Rowan, T.G., De Koning, H.P., Barrett, M.P., 2016. The animal trypanosomiasis and their chemotherapy: a review. *Parasitology* 143, 1862–1889.
- Goodwin, R., Bunch, J., McGinnity, D., 2017. Mass spectrometry imaging in oncology drug discovery. In: Drake, R.R., McDonnell, L.A. (Eds.), *Advances in Cancer Research*. Elsevier, pp. 133–171.
- Guengerich, F.P., 2011. Mechanisms of drug toxicity and relevance to pharmaceutical development. *Drug Metab. Pharmacokinet.* 26, 3–14.
- Gutteridge, J.M., 1985. Superoxide dismutase inhibits the superoxide-driven Fenton reaction at two different levels: implications for a wider protective role. *FEBS Lett.* 185, 19–23.
- Hall, B.S., Wu, X., Hu, L., Wilkinson, S.R., 2010. Exploiting the drug-activating properties of a novel trypanosomal nitroreductase. *Antimicrob. Agent. Chemother.* 54, 1193–1199.
- Hay, M., Thomas, D.W., Craighead, J.L., Economides, C., Rosenthal, J., 2014. Clinical investigation success rates for investigational drugs. *Nat. Biotechnol.* 32, 40–51.
- Hirumi, H., Hirumi, K., 1991. *In vitro* cultivation of *Trypanosoma congolense* bloodstream forms in the absence of feeder cell layers. *Parasitology* 102, 225–236.
- Horn, D., 2014. Antigenic variation in African trypanosomes. *Mol. Biochem. Parasitol.* 195, 123–129.
- Hu, X.-Z., Xu, Y., Yediler, A., 2007. Determinations of residual furazolidone and its metabolite, 3-amino-2-oxazolidinone (AOZ), in fish feeds by HPLC-UV and LC-MS/MS, respectively. *J. Agric. Food Chem.* 55, 1144–1149.
- Hughes, J.P., Rees, S., Kalindjian, S.B., Philpott, K.L., 2011. Principles of early drug discovery. *Br. J. Pharmacol.* 162, 1239–1249.
- Imran, M., Khan, S.A., Alshammari, M.K., Alqahtani, A.M., Alanazi, T.A., Kamal, M., Jawaid, T., Ghoneim, M.M., Alshehri, S., Shakeel, F., 2022. Discovery, development, inventions and patent review of fexinidazole: the first all-oral therapy for Human African Trypanosomiasis. *Pharmaceuticals* 15, 128.
- Ishiyama, M., Miyazono, Y., Sasamoto, K., Ohkura, Y., Ueno, K., 1997. A highly water-soluble disulfonated tetrazolium salt as a chromogenic indicator for NADH as well as cell viability. *Talanta* 44, 1299–1305.
- Kaiser, M., Mäser, P., Tadoori, L.P., Ioset, J.-R., Brun, R., 2015. Antiprotozoal activity profiling of approved drugs: a starting point toward drug repositioning. *PLoS One* 10, e0135556.
- Kasozi, K.I., MacLeod, E.T., Ntulume, I., Welburn, S.C., 2022. An update on African trypanocidal pharmaceuticals and resistance. *Front. Veterin. Sci.* 9, 828111.
- Katabazi, A., Aliero, A.A., Witto, S.G., Odoki, M., Musinguzi, S.P., 2021. Prevalence of *Trypanosoma congolense* and *Trypanosoma vivax* in Lira District, Uganda. *Biomed. Res. Int.* 2021.
- Katsuno, K., Burrows, J.N., Duncan, K., Van Huijsduijn, R.H., Kaneko, T., Kita, K., Mowbray, C.E., Schmatz, D., Warner, P., Slingsby, B., 2015. Hit and lead criteria in drug discovery for infectious diseases of the developing world. *Nat. Rev. Drug Discov.* 14, 751–758.
- Lipinski, C.A., Lombardo, F., Dominy, B.W., Feeney, P.J., 1997. Experimental and computational approaches to estimate solubility and permeability in drug discovery and development settings. *Adv. Drug Deliv. Rev.* 23, 3–25.
- Liu, S., Su, M., Song, S.-J., Jung, J.H., 2017. Marine-derived *Penicillium* species as producers of cytotoxic metabolites. *Mar. Drug.* 15, 329.
- Mercer, M.A., 2022. Nitrofurans Use in Animals. *MSD Veterinary Manual*.
- Molefe, N.I., Yamasaki, S., Macalanda, A.M.C., Suganuma, K., Watanabe, K., Xuan, X., Inoue, N., 2017. Oral administration of azithromycin ameliorates trypanosomiasis in *Trypanosoma congolense*-infected mice. *Parasitol. Res.* 116, 2407–2415.
- Morrison, L.J., Vezza, L., Rowan, T., Hope, J.C., 2016. Animal African trypanosomiasis: time to increase focus on clinically relevant parasite and host species. *Trend. Parasitol.* 32, 599–607.
- Muhanguzi, D., Picozzi, K., Hattendorf, J., Thrusfield, M., Kabasa, J.D., Waiswa, C., Welburn, S.C., 2014. The burden and spatial distribution of bovine African trypanosomes in small holder crop-livestock production systems in Tororo District, south-eastern Uganda. *Parasit. Vect.* 7, 603.
- Munsimbwe, L., Seetsi, A., Namangala, B., N'Da, D.D., Inoue, N., Suganuma, K., 2021. *In vitro* and *in vivo* trypanocidal efficacy of synthesized nitrofurantoin analogs. *Molecules* 26, 3372.
- Narita, K., Suganuma, K., Murata, T., Kondo, R., Satoh, H., Watanabe, K., Sasaki, K., Inoue, N., Yoshimura, Y., 2021. Synthesis and evaluation of trypanocidal activity of derivatives of naturally occurring 2, 5-diphenyloxazoles. *Bioorg. Med. Chem.* 42, 116253.

- Ndlovu, K., Kannigadu, C., Aucamp, J., van Rensburg, H.D.J., N'Da, D.D., 2023. Exploration of ethylene glycol linked nitrofurantoin derivatives against Leishmania: synthesis and *in vitro* activity. Arch. Pharm. (Weinheim), e2200529.
- Nok, A.J., 2009. African trypanosomiasis. In: Barrett, A.D., Stanberry, L.R. (Eds.), Vaccines For Biodefense and Emerging and Neglected Diseases. Academic Press, pp. 1258–1270.
- Nwaka, S., Hudson, A., 2006. Innovative lead discovery strategies for tropical diseases. Nat. Rev. Drug Discov. 5, 941–955.
- Paccamonti, D., Crabtree, J.R., 2019. Equine infertility and stud medicine practice. In: Noakes, D.E., Parkinson, T.J., England, G.C.W. (Eds.), Veterinary Reproduction and Obstetrics. Elsevier, pp. 541–580.
- Pays, E., Radwanska, M., Magez, S., 2023. The pathogenesis of african trypanosomiasis. Ann. Rev. Pathol.: Mechn. Dis. 18, 19–45.
- Peregrine, A., Mamman, M., 1993. Pharmacology of diminazene: a review. Acta Trop. 54, 185–203.
- Raaflaub, J., 1980. The bioavailability of orally administered drugs with special regard to the liver as a filter for foreign matter. Schweiz. Med. Wochenschr. 110, 354–362.
- Roldán, M.D., Pérez-Reinado, E., Castillo, F., Moreno-Vivián, C., 2008. Reduction of polynitroaromatic compounds: the bacterial nitroreductases. FEMS Microbiol. Rev. 32, 474–500.
- Royle, K.E., del Val, I.J., Kontoravdi, C., 2013. Integration of models and experimentation to optimise the production of potential biotherapeutics. Drug Discov. Today 18, 1250–1255.
- Ryan, A., 2017. Azoreductases in drug metabolism. Br. J. Pharmacol. 174, 2161–2173.
- Sahoo, B.M., Ravi Kumar, B., Sruti, J., Mahapatra, M.K., Banik, B.K., Borah, P., 2021. Drug repurposing strategy (DRS): emerging approach to identify potential therapeutics for treatment of novel coronavirus infection. Front. Mol. Biosci. 8.
- Salas, C.O., Faúndez, M., Morello, A., Maya, J.D., Tapia, R.A., 2011. Natural and synthetic naphthoquinones active against Trypanosoma cruzi: an initial step towards new drugs for Chagas disease. Curr. Med. Chem. 18, 144–161.
- Shaw, A., Wint, G., Cecchi, G., Torr, S., Mattioli, R., Robinson, T.P., 2015. Mapping the benefit-cost ratios of interventions against bovine trypanosomiasis in Eastern Africa. Prev. Vet. Med. 122, 406–416.
- Sokolova, A.Y., Wyllie, S., Patterson, S., Oza, S.L., Read, K.D., Fairlamb, A.H., 2010. Cross-resistance to nitro drugs and implications for treatment of human African trypanosomiasis. Antimicrob. Agent. Chemother. 54, 2893–2900.
- Spitzer, M., Sabadini, E., Loh, W., 2002. Poly (ethylene glycol) or Poly (ethylene oxide)?: magnitude of end-group Contribution to the Partitioning of Ethylene Oxide Oligomers and Polymers between Water and Organic Phases. J. Braz. Chem. Soc. 13, 7–9.
- Stocks, M., 2013. The Small Molecule Drug Discovery Process—From Target Selection to Candidate selection, Introduction to Biological and Small Molecule Drug Research and Development. Elsevier, pp. 81–126.
- Suganuma, K., Allamanda, P., Hakimi, H., Zhou, M., Angeles, J.M., Kawazu, S.-i., Inoue, N., 2014. Establishment of ATP-based luciferase viability assay in 96-well plate for Trypanosoma congolense. J. Vet. Med. Sci. 76, 1437–1441.
- Suganuma, K., N'Da, D.D., Watanabe, K.-i., Tanaka, Y., Mossaad, E., Elata, A., Inoue, N., Kawazu, S.-i., 2022. Therapeutic efficacy of orally administered nitrofurantoin against animal African trypanosomiasis caused by Trypanosoma congolense infection. Pathogens 11, 331.
- Suganuma, K., Narantsatsral, S., Battur, B., Yamasaki, S., Otgonsuren, D., Musinguzi, S. P., Davaasuren, B., Battsetseg, B., Inoue, N., 2016. Isolation, cultivation and molecular characterization of a new Trypanosoma equiperdum strain in Mongolia. Parasit Vect. 9, 1–9.
- Suganuma, K., Yamasaki, S., Molefe, N.I., Musinguzi, P.S., Davaasuren, B., Mossaad, E., Narantsatsral, S., Battur, B., Battsetseg, B., Inoue, N., 2017. The establishment of *in vitro* culture and drug screening systems for a newly isolated strain of Trypanosoma equiperdum. Int. J. Parasitol.: Drug. Drug Resist. 7, 200–205.
- Swallow, B., 2000. Impacts of Trypanosomiasis on African Agriculture. Food and Agriculture Organization of the United Nations.
- Teoh, X.-Y., bt Mahyuddin, F.N., Ahmad, W., Chan, S.-Y., 2020. Formulation strategy of nitrofurantoin: co-crystal or solid dispersion? Pharm. Dev. Technol. 25, 245–251.
- Thompson, M., Vadala, T., Vadala, M., Lin, Y., Riffle, J., 2008. Synthesis and applications of heterobifunctional poly (ethylene oxide) oligomers. Polym. (Guildf) 49, 345–373.
- Tominaga, H., Ishiyama, M., Ohseto, F., Sasamoto, K., Hamamoto, T., Suzuki, K., Watanabe, M., 1999. A water-soluble tetrazolium salt useful for colorimetric cell viability assay. Anal. Commun. 36, 47–50.
- Trukhacheva, L., Grigor'ev, N., Arzamastsev, A., Granik, V., 2005. Hydrolytic and reductive transformations of nifuroxazide. Pharm. Chem. J. 39, 381–384.
- Vadala, M., Thompson, M., Ashworth, M., Lin, Y., Vadala, T., Ragheb, R., Riffle, J., 2008. Heterobifunctional poly (ethylene oxide) oligomers containing carboxylic acids. Biomacromolecules 9, 1035–1043.
- Van De Waterbeemd, H., Gifford, E., 2003. ADMET in silico modelling: towards prediction paradise? Nat. Rev. Drug Discov. 2, 192–204.
- Vanhamme, L., Paturiaux-Hanocq, F., Poelvoorde, P., Nolan, D.P., Lins, L., Van Den Abbeele, J., Pays, A., Tebabi, P., Van Xong, H., Jacquet, A., 2003. Apolipoprotein LI is the trypanosome lytic factor of human serum. Nature 83–87.
- Vass, M., Hruska, K., Franek, M., 2008. Nitrofurantoin antibiotics: a review on the application, prohibition and residual analysis. Vet. Med. (Praha) 53, 469.
- Veber, D.F., Johnson, S.R., Cheng, H.-Y., Smith, B.R., Ward, K.W., Kopple, K.D., 2002. Molecular properties that influence the oral bioavailability of drug candidates. J. Med. Chem. 45, 2615–2623.
- Venturelli, A., Tagliacuzzi, L., Lima, C., Venuti, F., Malpezzi, G., Magoulas, G.E., Santarem, N., Calogeropoulou, T., Cordeiro-da-Silva, A., Costi, M.P., 2022. Current treatments to control African trypanosomiasis and one health perspective. Microorganisms 10, 1298.
- Vera, B., Vázquez, K., Mascayano, C., Tapia, R.A., Espinosa, V., Soto-Delgado, J., Salas, C. O., Paulino, M., 2017. Structural analysis and molecular docking of trypanocidal aryloxy-quinones in trypanothione and glutathione reductases: a comparison with biochemical data. J. Biomol. Struct. Dyn. 35, 1785–1803.
- Waldman, S.A., 2002. Does potency predict clinical efficacy? Illustration through an antihistamine model. Ann. Allergy Asthma Immunol. 89, 7–12.
- Walzer, P.D., Kim, C.K., Foy, J., Zhang, J., 1991. Furazolidone and nitrofurantoin in the treatment of experimental Pneumocystis carinii pneumonia. Antimicrob. Agents Chemother. 35, 158–163.
- Wardman, P., 1985. Some reactions and properties of nitro radical-anions important in biology and medicine. Environ. Health Perspect. 64, 309–320.
- Weisman, J.L., Liou, A.P., Shelat, A.A., Cohen, F.E., Kiplin Guy, R., DeRisi, J.L., 2006. Searching for new antimalarial therapeutics amongst known drugs. Chem. Biol. Drug Des. 67, 409–416.
- WHO, 2023. Trypanosomiasis, Human African (Sleeping Sickness). WHO Fact Sheet.
- Wilkowsky, S.E., 2022. Trypanosomiasis in Animals. MSD Veterinary Manual.
- Zhan, P., Yu, B., Ouyang, L., 2022. Drug repurposing: an effective strategy to accelerate contemporary drug discovery. Drug Discov. Today 27, 1785–1788.
- Zhou, L., Ishizaki, H., Spitzer, M., Taylor, K.L., Temperley, N.D., Johnson, S.L., Brear, P., Gautier, P., Zeng, Z., Mitchell, A., 2012. ALDH2 mediates 5-nitrofurantoin activity in multiple species. Chem. Biol. 19, 883–892.
- Zuma, N.H., Aucamp, J., David, D.D., 2019. An update on derivatisation and repurposing of clinical nitrofurantoin drugs. Eur. J. Pharm. Sci. 140, 105092.
- Zuma, N.H., Aucamp, J., van Rensburg, H.D.J., David, D.D., 2023. Synthesis and *in vitro* antileishmanial activity of alkylene-linked nitrofurantoin-triazole hybrids. Eur. J. Med. Chem. 246, 115012.
- Zuma, N.H., Aucamp, J., Viljoen, M., N'Da, D.D., 2022. Synthesis, *in vitro* Antileishmanial Efficacy and Hit/Lead Identification of Nitrofurantoin-Triazole Hybrids. ChemMedChem 17, e202200023.
- Zuma, N.H., Smit, F.J., Seldon, R., Aucamp, J., Jordaan, A., Warner, D.F., David, D.D., 2020. Single-step synthesis and *in vitro* anti-mycobacterial activity of novel nitrofurantoin analogues. Bioorg. Chem. 96, 103587.